平面设计软件在科研图像处理中的应用

胡萍　邮箱：hupin@fudan.edu.cn
复旦大学图书馆 · 复旦大学人文社科数据研究所

Welcome

欢迎大家参加本次的线上培训课程。

欢迎大家多与我交流、讨论、共同学习。

图形图像处理学习讨论群

一位***Science***杂志编辑说过：“我通常审阅一篇文章只用1分钟。”

在如此短暂的时间里，想脱颖而出，论文配图直接影响文章质量。

目录

contents

科学可视化的属性

科学可视化，就是利用计算机将符号形式转变为图形图像的形式来帮助人们理解和在视觉上理清数据中的内在关系。

人们认识事物是一个综合运用视觉、听觉、嗅觉、触觉和抽象思维能力的复杂过程，其中视觉是人们获取信息的最重要、最快速的途径。

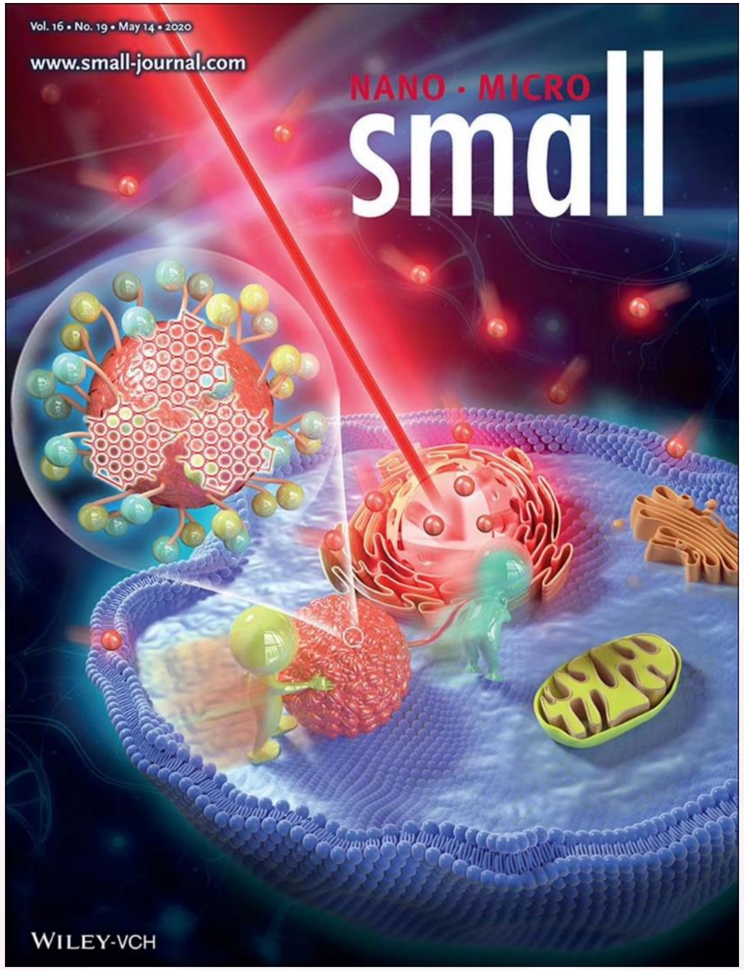

科学可视化的属性

科学可视化（Scientific visualization），是科学中一个跨学科研究与应用的领域，如建筑学、气象学、医学、生命科学、先进材料、大数据等方面。

科学可视化包括图像理解和图像生成两个部分。

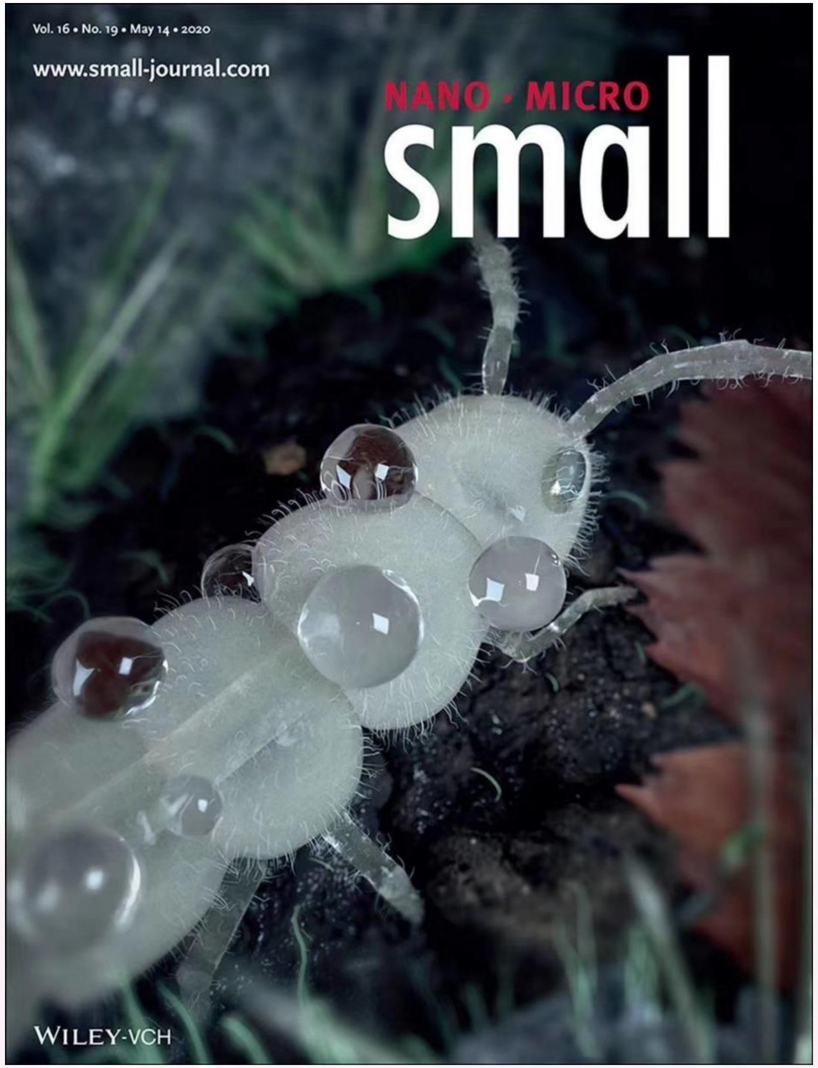

科学可视化重要体现在以下几个方面：

- 人机协同处理。
- 科研成果的信息表达。
- 复杂数据的可视化处理、研究成果的可视化表达。
- 为各大领域提供分析工具与手段。

当科学遇见艺术……

我们越来越发现很多大刊的整体感觉越发精美了，除了对科研论文的相关高要求外，很多杂志编辑对于文章的整体美感，包括版式的分布、插图的制作水平，还有一些封面稿件的设计制作水准，我仔细品味，有相当高的艺术水平。对于画面的视觉整体构思、构图、色调、空间虚实的处理手法，单从艺术的视角来看，都是非常考究的。

可视化图像分类

- 以表现手法为依据
- 以绘制原理为依据

可视化图像分类

摄影风格

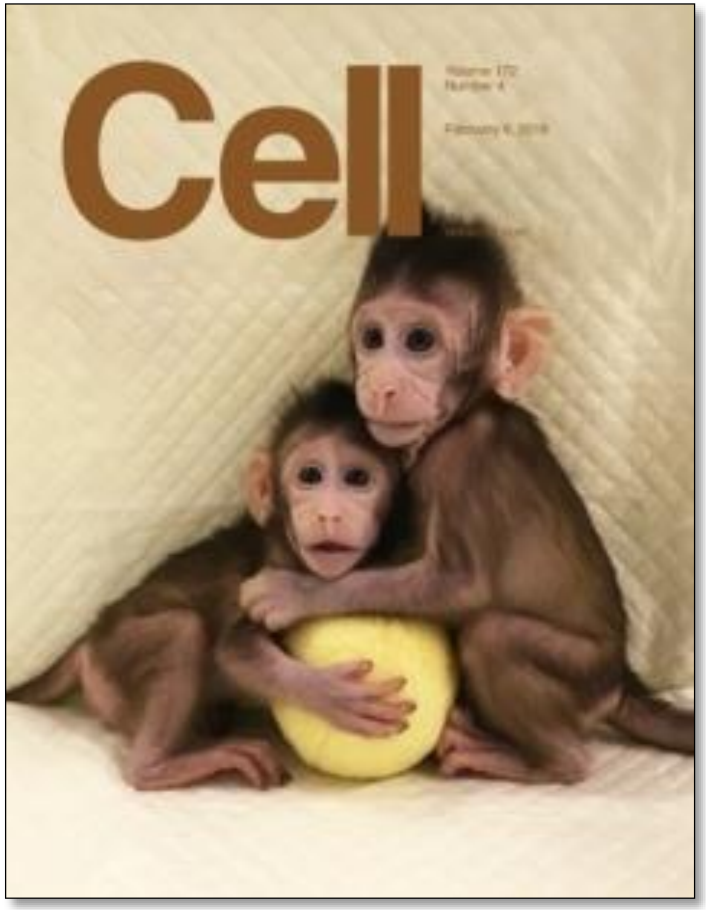

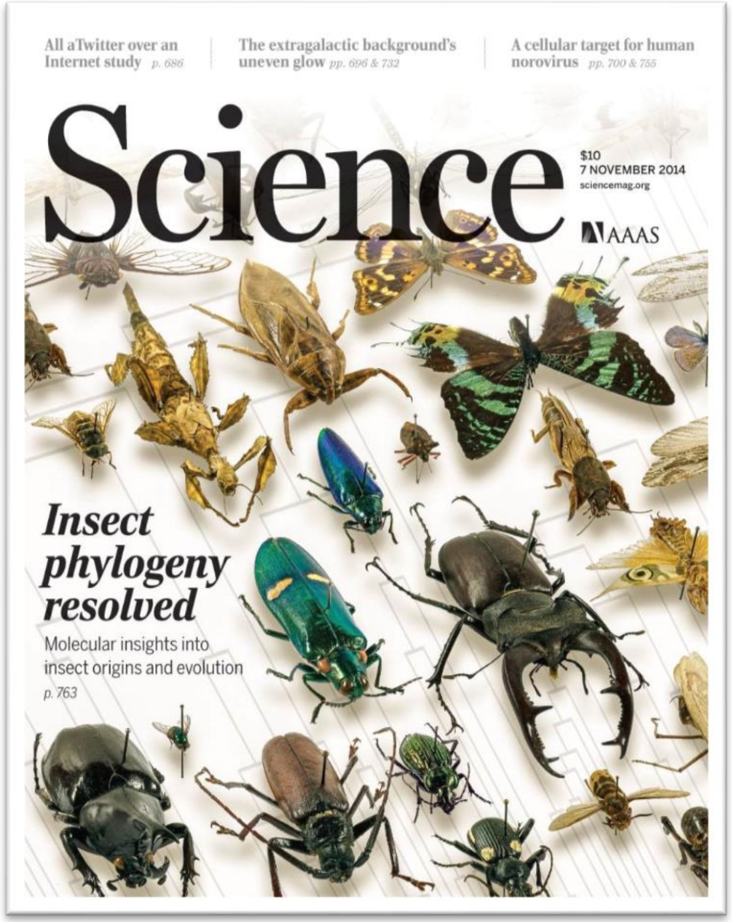

可视化图像分类

三维风格

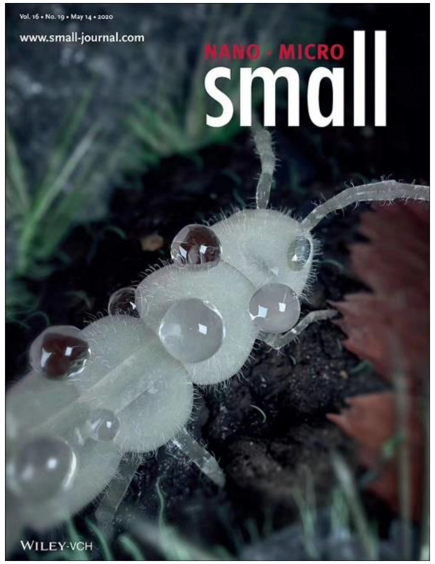

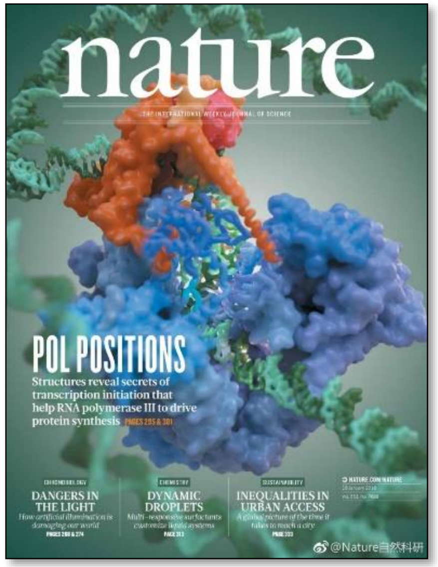

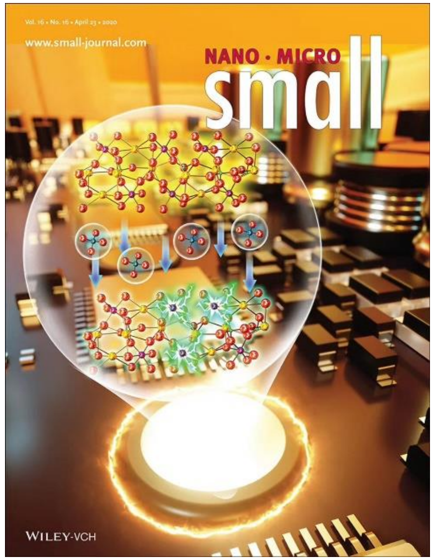

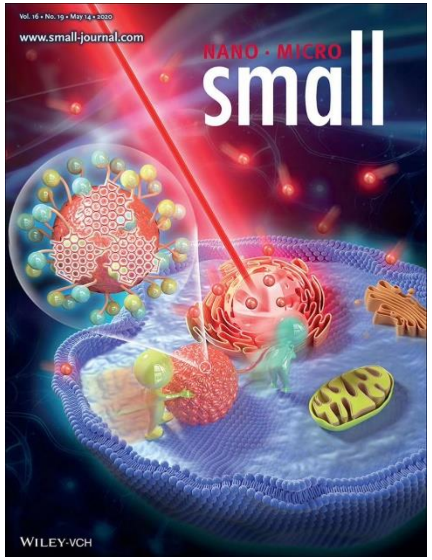

平面风格

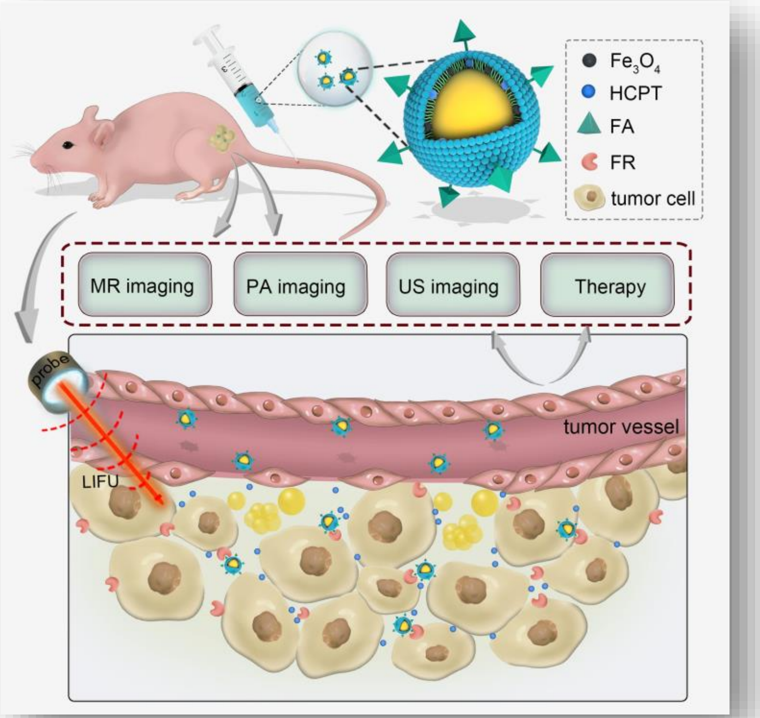
Fe3O4
HCPT
FA
FR
tumor cell
MR imaging
PA imaging
US imaging
Therapy
probe
tumor vessel
LIFU

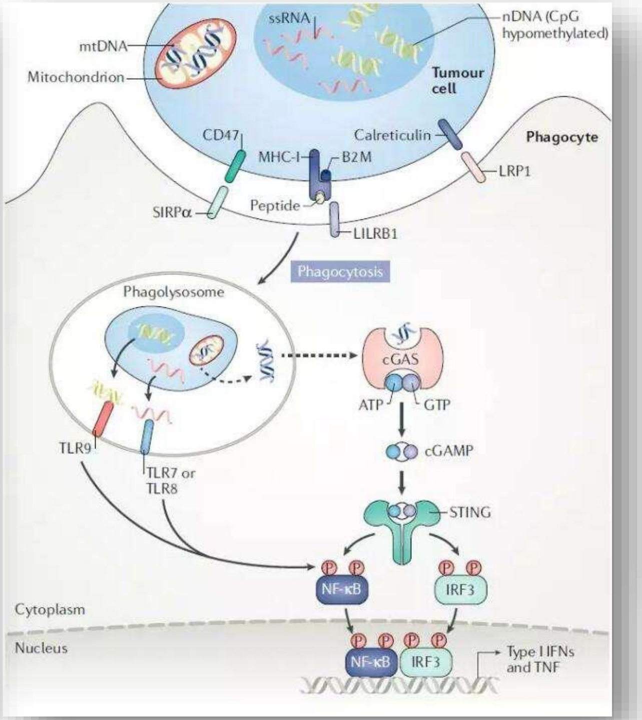
mtDNA
Mitochondrion
ssRNA
nDNA (CpG hypomethylated)
Tumour cell
CD47
MHC-I
B2M
Calreticulin
Phagocyte
LRP1
SIRPα
Peptide
LILRB1
Phagocytosis
Phagolysosome
cGAS
ATP
GTP
cGAMP
STING
TLR9
TLR7 or TLR8
NF-κB
IRF3
Cytoplasm
Nucleus
Type I IFNs and TNF

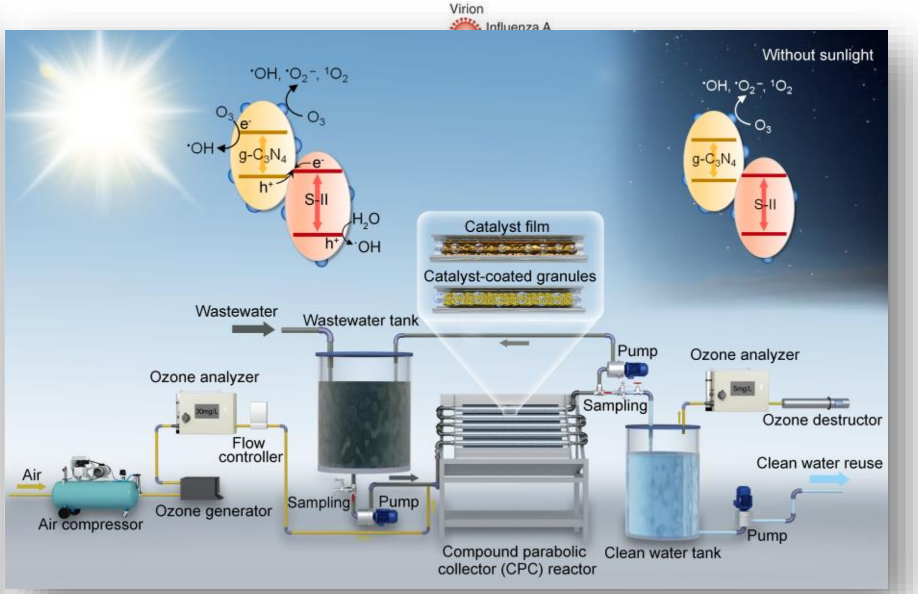
Without sunlight
Catalyst film
Catalyst-coated granules
Wastewater
Wastewater tank
Pump
Ozone analyzer
Sampling
Ozone destructor
Flow controller
Clean water reuse
Air
Air compressor
Ozone generator
Compound parabolic collector (CPC) reactor
Clean water tank

平面风格

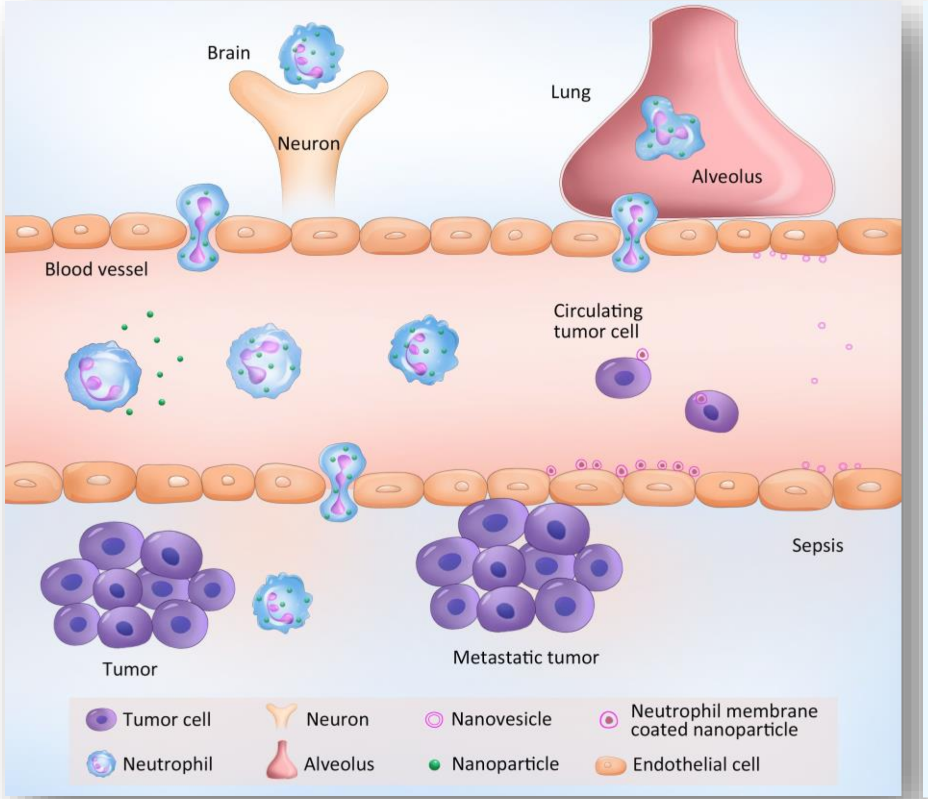
Brain
Lung
Neuron
Alveolus
Blood vessel
Circulating tumor cell
Sepsis
Tumor
Metastatic tumor
Tumor cell
Neuron
Nanovesicle
Neutrophil membrane coated nanoparticle
Neutrophil
Alveolus
Nanoparticle
Endothelial cell

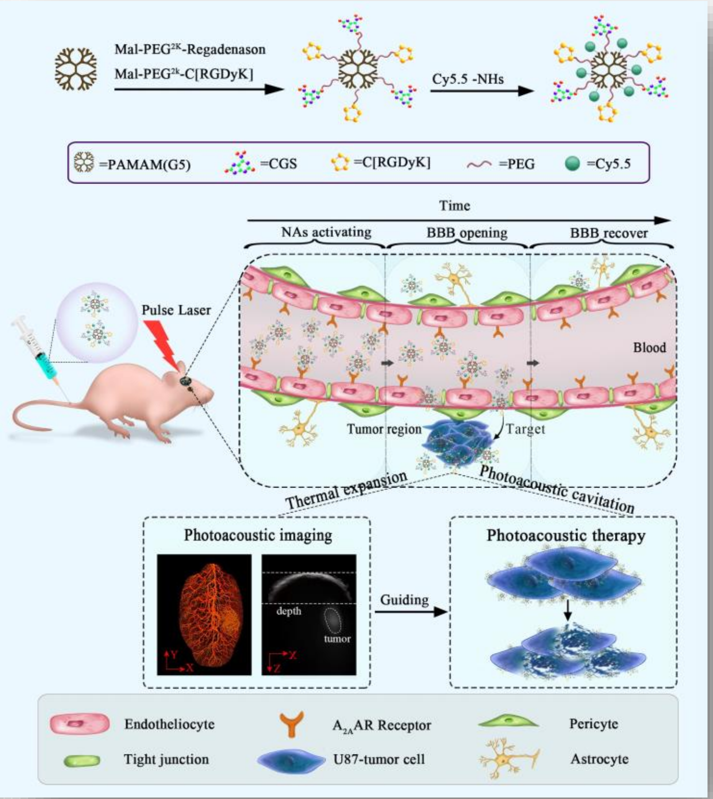
Mal-PEG2K-Regadenason
Mal-PEG2K-C[RGDyK]
Cy5.5 -NHs
=PAMAM(G5)
=CGS
=C[RGDyK]
=PEG
=Cy5.5
Time
NAs activating
BBB opening
BBB recover
Pulse Laser
Blood
Tumor region
Target
Thermal expansion
Photoacoustic cavitation
Photoacoustic imaging
Guiding
Photoacoustic therapy
depth
tumor
Endotheliocyte
Tight junction
A2AAR Receptor
U87-tumor cell
Pericyte
Astrocyte

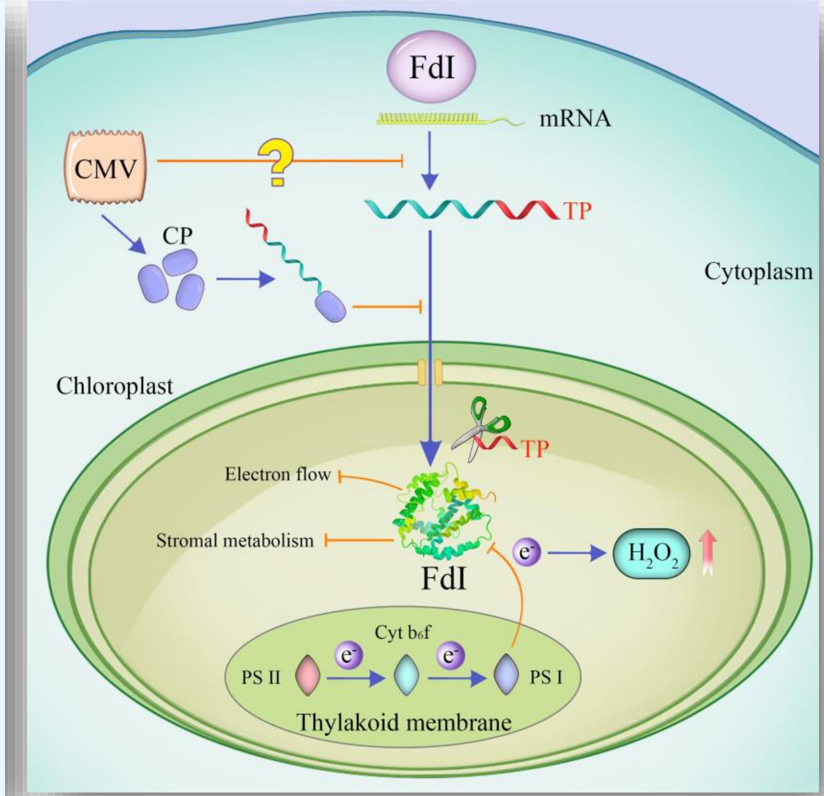
FdI
mRNA
CMV
CP
TP
Cytoplasm
Chloroplast
Electron flow
Stromal metabolism
FdI
H2O2
Cyt b6f
PS II
PS I
Thylakoid membrane

可视化图像分类

国画风格

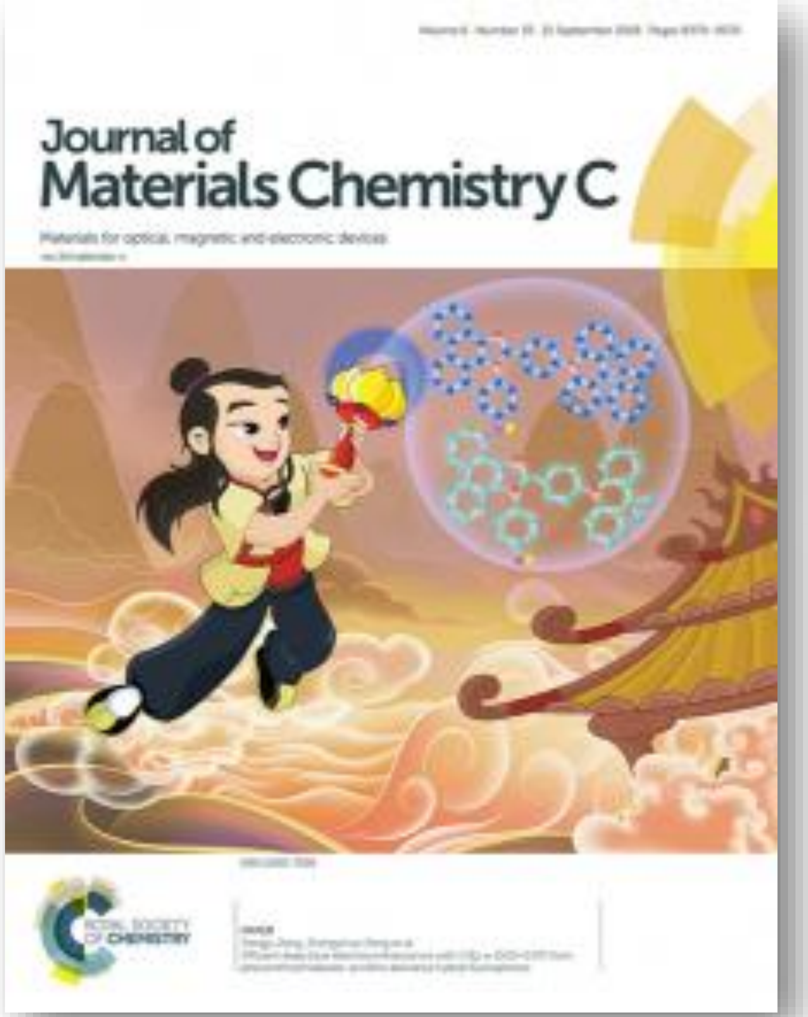

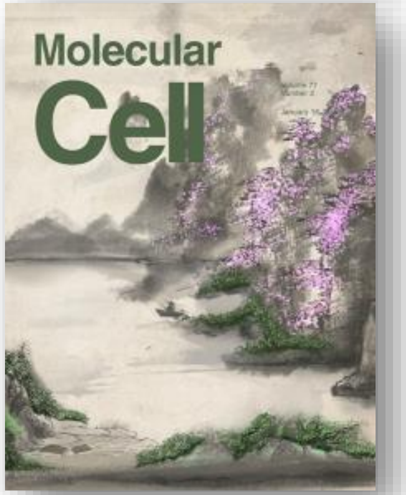

常用平面软件简介

Photoshop

illustrator

Indesign

常用平面软件简介

PS，是由Adobe开发和发行的图像处理软件。

Photoshop主要处理以像素所构成的数字图像。使用其众多的编修与绘图工具，可以有效地进行图片编辑工作。ps有很多功能，在图像、图形、文字、视频、出版等各方面都有涉及。

常用平面软件简介

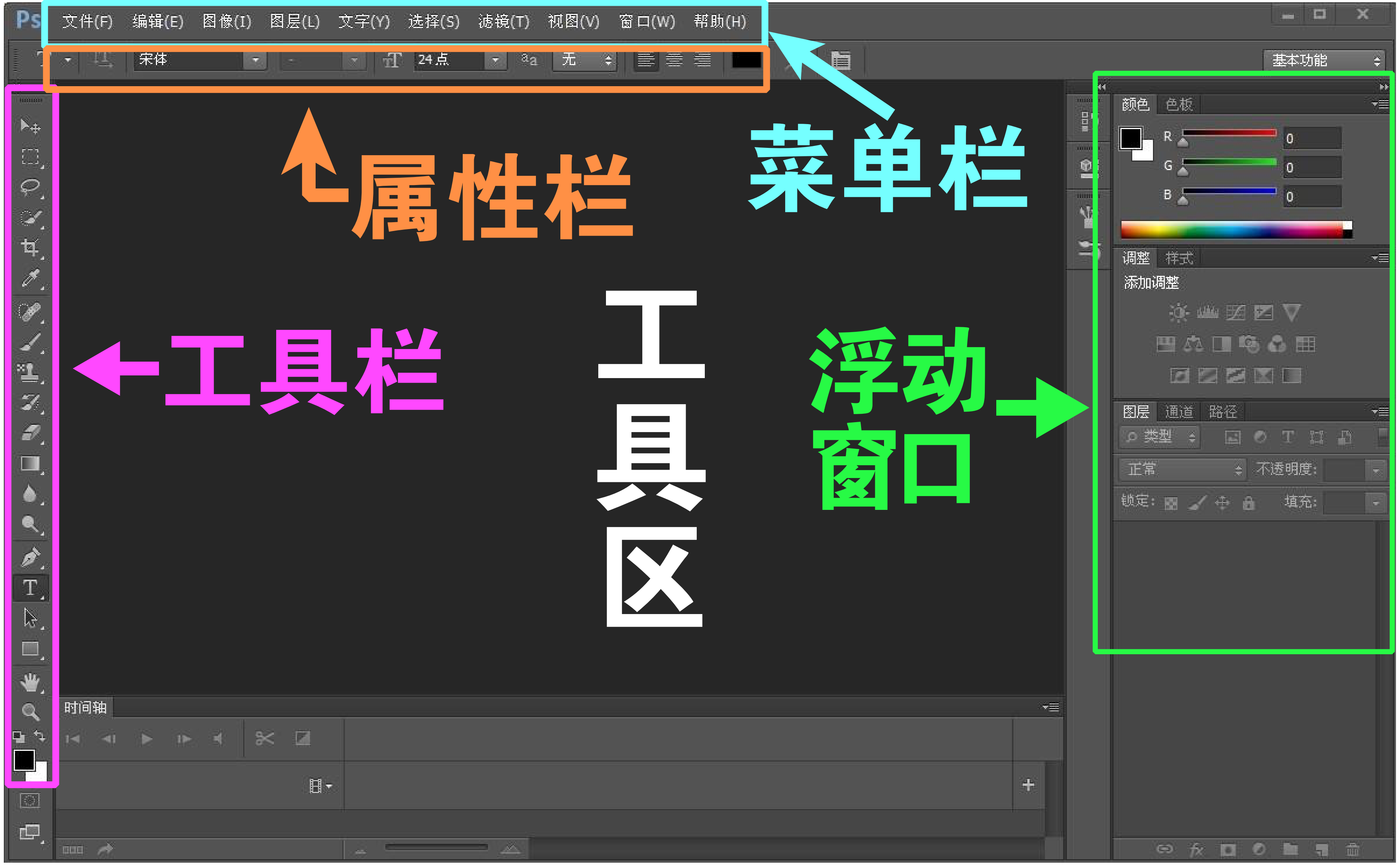

文件(F) 编辑(E) 图像(I) 图层(L) 文字(Y) 选择(S) 滤镜(T) 视图(V) 窗口(W) 帮助(H)
宋体
24 点
无
基本功能
属性栏
菜单栏
工具栏
工具区
浮动窗口
颜色 色板
调整 样式
添加调整
图层 通道 路径
类型
正常
不透明度:
锁定:
填充:
时间轴

常用平面软件简介

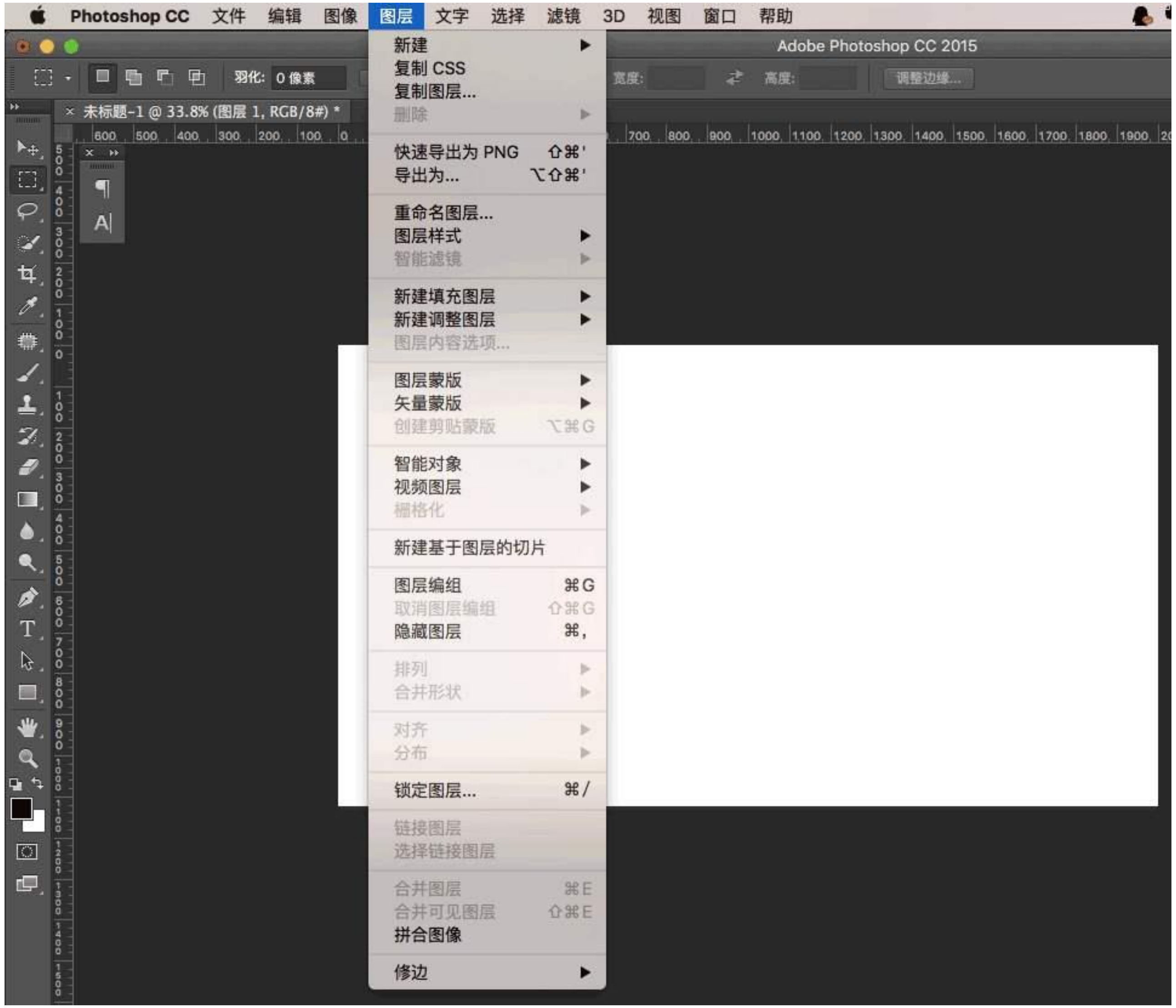

Photoshop CC
文件
编辑
图像
图层
文字
选择
滤镜
3D
视图
窗口
帮助
Adobe Photoshop CC 2015
未标题-1 @ 33.8% (图层 1, RGB/8#) *
新建
复制 CSS
复制图层...
删除
快速导出为 PNG ⇧⌘'
导出为... ⌥⇧⌘'
重命名图层...
图层样式
智能滤镜
新建填充图层
新建调整图层
图层内容选项...
图层蒙版
矢量蒙版
创建剪贴蒙版 ⌥⌘G
智能对象
视频图层
栅格化
新建基于图层的切片
图层编组 ⌘G
取消图层编组 ⇧⌘G
隐藏图层 ⌘,
排列
合并形状
对齐
分布
锁定图层... ⌘/
链接图层
选择链接图层
合并图层 ⌘E
合并可见图层 ⇧⌘E
拼合图像
修边

常用平面软件简介


Photoshop CC 文件 编辑 图像 图层 文字 选择 滤镜 3D 视图 窗口 帮助
Adobe Photoshop CC 2019
Nipic_24626866_20191106125053281036.psd @ 91.6%(CMYK/8*) *
EASYBRANDZ PRESENTS
SAT 29 JUL
BLACK PARTY
OPENING DJ ANDY
IN THE LOUNGE
DJ MOUSE
$30 FEE ADMISSION / DOORS OPEN AT 22:00 HOURS
FACEBOOK.COM/CLUBNAME
TWITTER.COM/CLUBNAME
图层

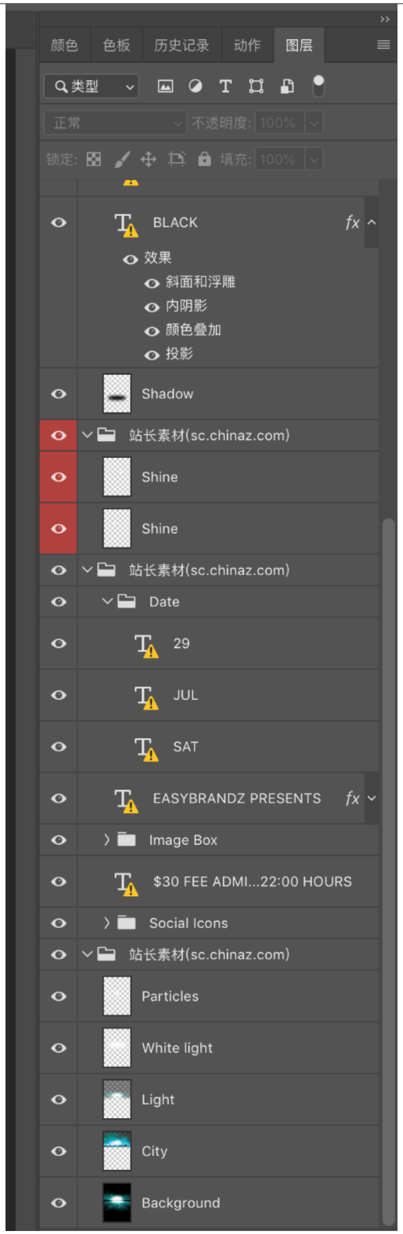
颜色 色板 历史记录 动作 图层
BLACK
效果
斜面和浮雕
内阴影
颜色叠加
投影
Shadow
站长素材(sc.chinaz.com)
Shine
Shine
站长素材(sc.chinaz.com)
Date
29
JUL
SAT
EASYBRANDZ PRESENTS
Image Box
$30 FEE ADMI...22:00 HOURS
Social Icons
站长素材(sc.chinaz.com)
Particles
White light
Light
City
Background


颜色 色板 历史记录 动作 图层
正常
溶解
变暗
正片叠底
颜色加深
线性加深
深色
变亮
滤色
颜色减淡
线性减淡（添加）
浅色
叠加
柔光
强光
亮光
线性光
点光
实色混合
差值
排除
减去
划分
色相
饱和度
颜色
明度
不透明度: 100%
填充: 100%
效果
斜面和浮雕
内阴影
颜色叠加
投影
Shadow
站长素材(sc.chinaz.com)
Shine
Shine
站长素材(sc.chinaz.com)
Date
29
JUL

特效

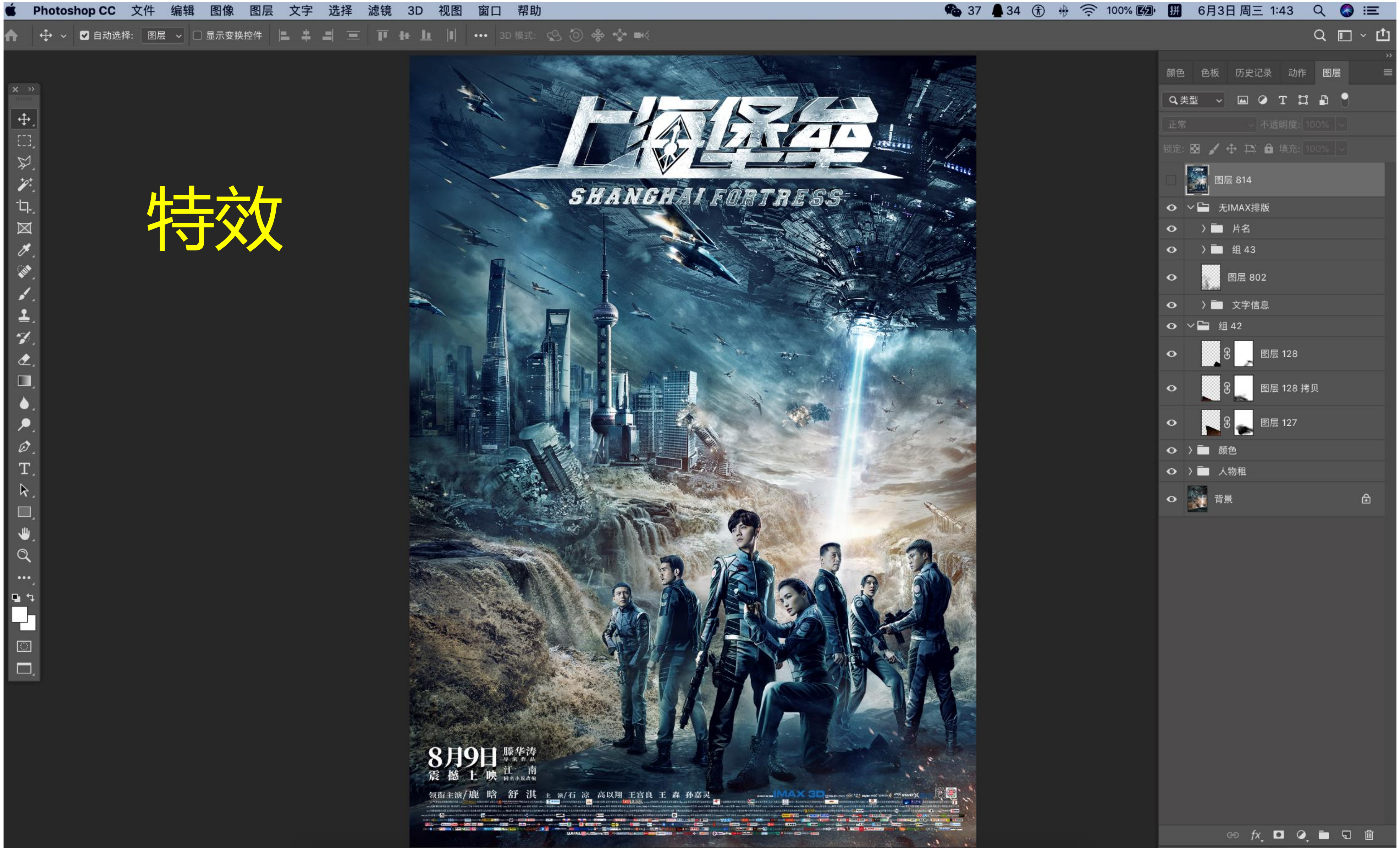
Photoshop CC
文件
编辑
图像
图层
文字
选择
滤镜
3D
视图
窗口
帮助
6月3日 周三 1:43
自动选择:
图层
显示变换控件
上海堡垒
SHANGHAI FORTRESS
8月9日
震撼上映
颜色
色板
历史记录
动作
图层
图层 814
无IMAX排版
片名
组 43
图层 802
文字信息
组 42
图层 128
图层 128 拷贝
图层 127
颜色
人物租
背景

Illustrator（插图画家）

Adobe illustrator，常被称为“AI”，是一种应用于出版、多媒体和在线图像的工业标准矢量插画的软件。

作为一款非常好用的矢量图形处理工具，几乎是平面设计师吃饭的最重要的家伙，这个软件主要应用于印刷出版、海报、书籍排版、专业插画、多媒体图像处理和互联网页面的制作等，也可以为线稿提供较高的精度和控制，适合生产任何小型设计到大型的复杂项目。

常用平面软件简介

常用平面软件简介


Illustrator CC 文件 编辑 对象 文字 选择 效果 视图 窗口 帮助
Shanghai
BDJI
Science & Research
上海市科研领域大数据联合
拼合器预览
描边 ⌘F10
文字
文档信息
渐变 ⌘F9
特性 ⌘F11
画板
画笔 F5
符号 ⇧⌘F11
色板
资源导出
路径查找器 ⇧⌘F9
透明度 ⇧⌘F10
链接
颜色 F6
颜色主题
颜色参考 ⇧F3
魔棒
图形样式库
画笔库
符号库
色板库
2020读书节.ai* @ 16.67% (RGB/GPU 预览)
大数据实验室logo.ai* @ 50% (RGB/GPU 预览)
未标题-2.ai* @ 25% (RGB/GPU 预览)
未标题-3* @ 200% (RGB/GPU 预览)
VisiBone2
Web
中性
儿童物品
公司
图案
大地色调
庆祝
渐变
科学
系统 (Macintosh)
系统 (Windows)
纺织品
肤色
自然
色标簿
艺术史
金属
颜色属性
食品
默认色板
用户定义
其它库...
ANPA Color
DIC Color Guide
FOCOLTONE
HKS E
HKS E Process
HKS K
HKS K Process
HKS N
HKS N Process
HKS Z
HKS Z Process
PANTONE+ CMYK Coated
PANTONE+ CMYK Uncoated
PANTONE+ Color Bridge Coated
PANTONE+ Color Bridge Uncoated
PANTONE+ Metallic Coated
PANTONE+ Pastels & Neons Coated
PANTONE+ Pastels & Neons Uncoated
PANTONE+ Premium Metallics Coated
PANTONE+ Solid Coated
PANTONE+ Solid Uncoated
TOYO 94 COLOR FINDER
TOYO Color Finder
TRUMATCH

常用平面软件简介

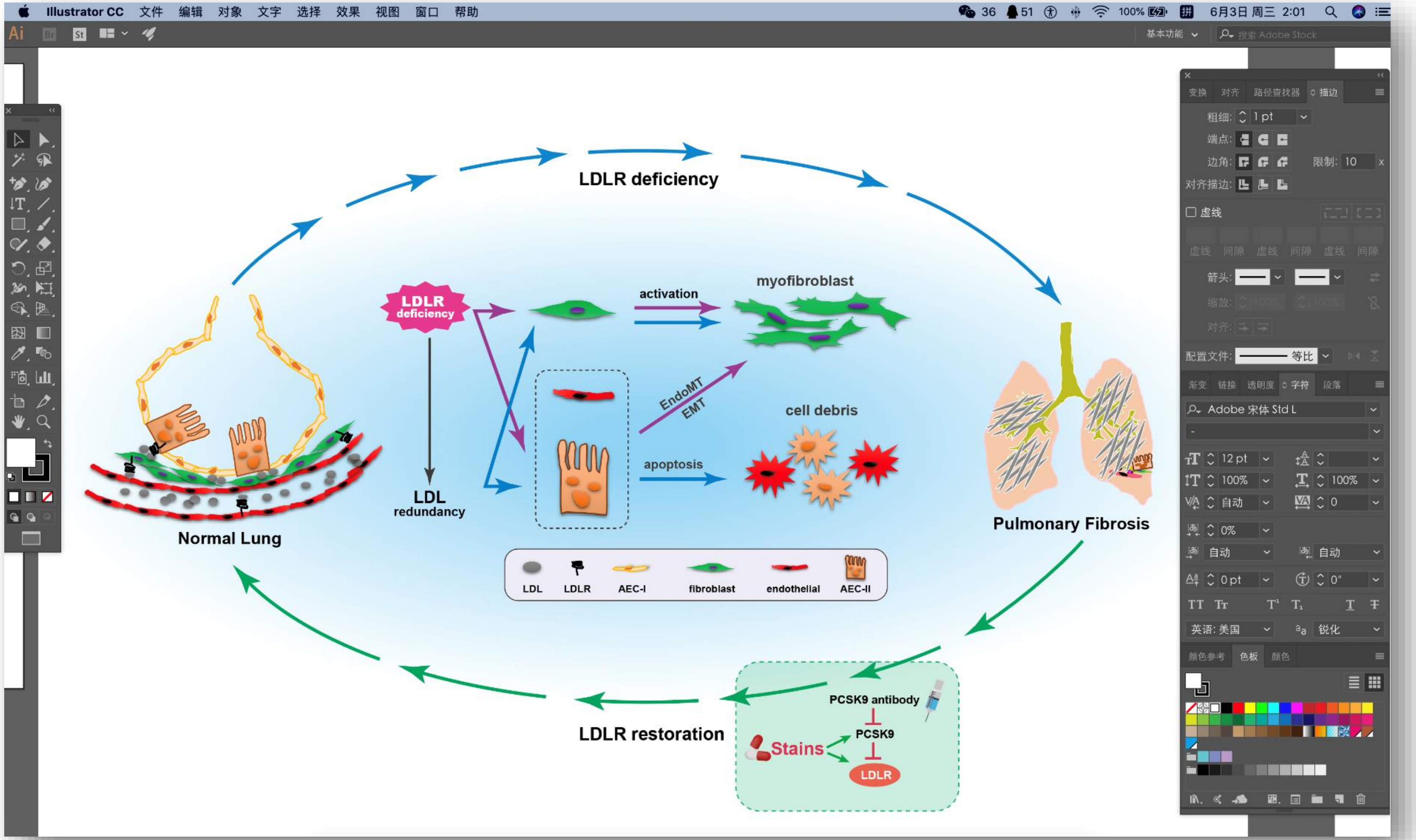

LDLR deficiency
LDLR deficiency
activation
myofibroblast
EndoMT
EMT
cell debris
apoptosis
LDL redundancy
Normal Lung
Pulmonary Fibrosis
LDL
LDLR
AEC-I
fibroblast
endothelial
AEC-II
PCSK9 antibody
PCSK9
Stains
LDLR
LDLR restoration

Indesign

Adobe InDesign是Adobe公司的一个 桌面出版 (DTP) 的应用程序，主要用于各种印刷品的排版编辑。我们做杂志编辑或者文本设计排版的一款软件是PageMaker，后来这款软件被Indesign所替代，IDesign可以将文档直接导出为Adobe的PDF格式，跟印刷输出对接的功能非常好，色彩还原功能非常优秀。

常用平面软件简介

3Dmax

Maya

科研论文图像常用的几种图形格式

矢量图：

所谓矢量图，就是使用直线和曲线来描述的图形，构成这些图形的元素是一些点、线、矩形、多边形、圆和弧线等，它们都是通过数学公式计算获得的，具有编辑后不失真的特点。

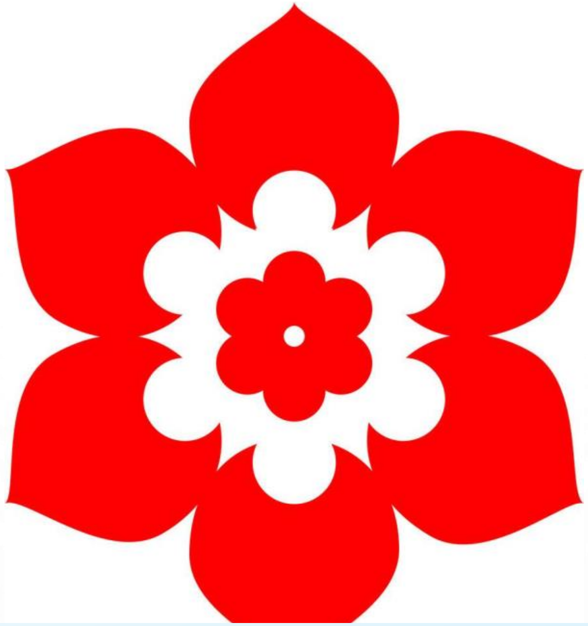

位图：

位图图像，亦称为点阵图像或栅格图像，是由称作像素（图片元素）的单个点组成的。这些点可以进行不同的排列和染色以构成图样。当放大位图时，可以看见赖以构成整个图像的无数单个方块。扩大位图尺寸的效果是增大单个像素，从而使线条和形状显得参差不齐。

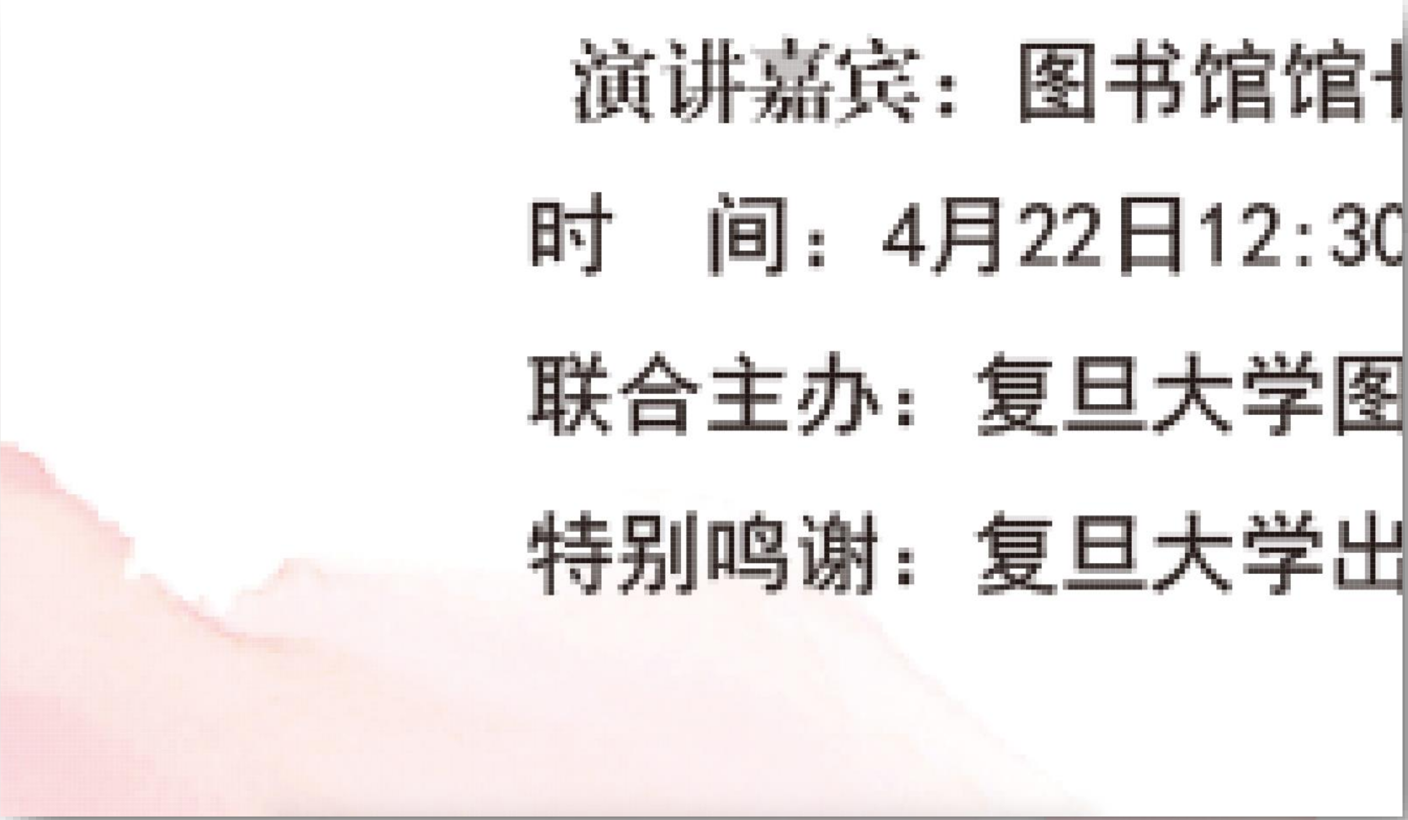
演讲嘉宾：图书馆馆
时　间：4月22日12:30
联合主办：复旦大学图
特别鸣谢：复旦大学出

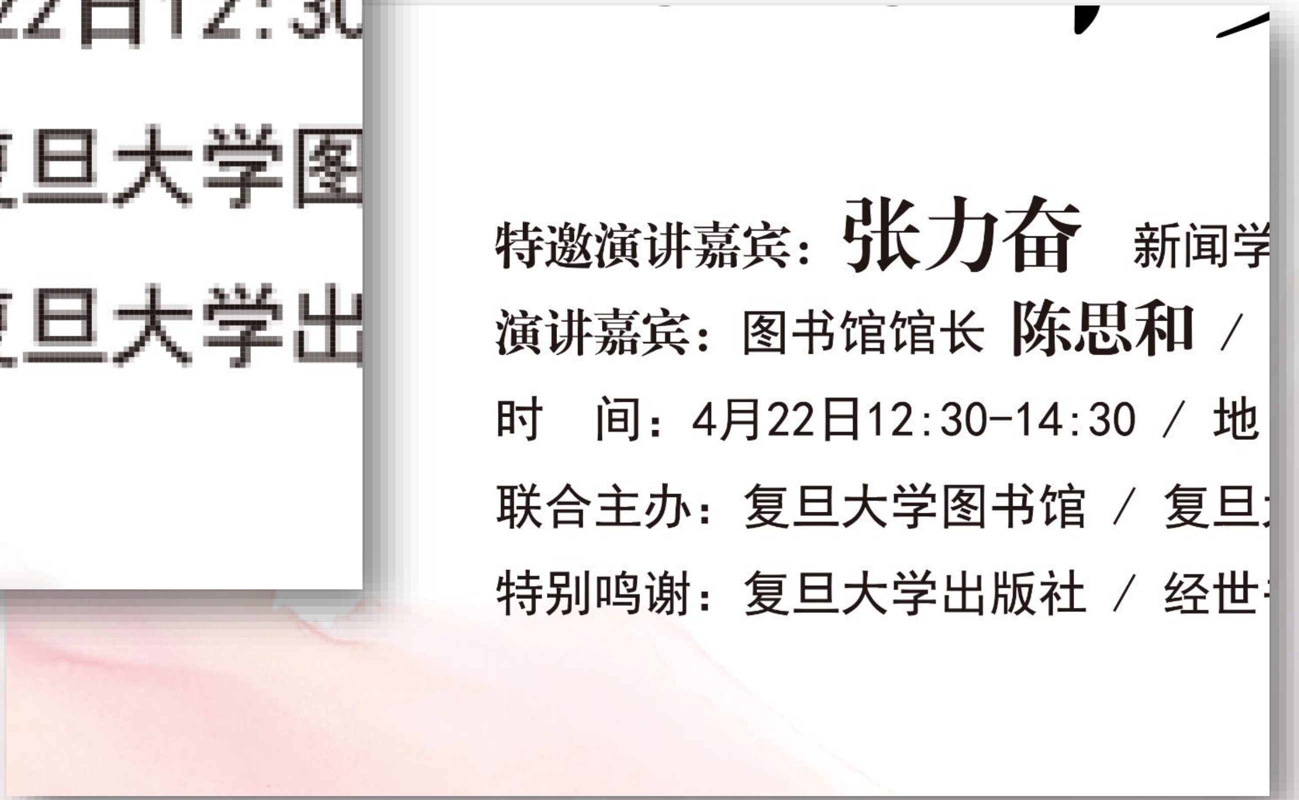
特邀演讲嘉宾：张力奋　新闻学
演讲嘉宾：图书馆馆长 陈思和 /
时　间：4月22日12:30-14:30 / 地
联合主办：复旦大学图书馆 / 复旦
特别鸣谢：复旦大学出版社 / 经世

科研论文图像常用的几种图形格式

在介绍文件格式之前，首先要明确作图的用途，不同的用途对应不同的文件格式。

格式	特点
jpg	有损压缩格式，可将文件的容量缩小几十倍，对图片的色彩质量造成一定损失，不支持多图层。
tif	无损压缩格式，可将文件容量缩小2～3倍，可保留图形的细节，因此是制版印刷行业优先选择的图形格式。

科研论文图像常用的几种图形格式

格式	特点
eps	EPS文件是目前桌面印刷系统普遍使用的通用交换格式当中的一种综合格式又被称为带有预视图象的PS格式。
pdf	PDF 文件是以PostScript语言图象模型为基础，无论在哪种打印机上都可保证精确的颜色和准确的打印效果 。集成度和安全可靠性都较高。

格式	特点
psd	PSD格式是Adobe Photoshop软件自身的格式，这种格式可以存储Photoshop中所有信息，便于修改加工。
ai	ai格式是Adobe公司发布的矢量软件illustrator的专用文件格式。它的优点是占用硬盘空间小，打开速度快，方便格式转换。

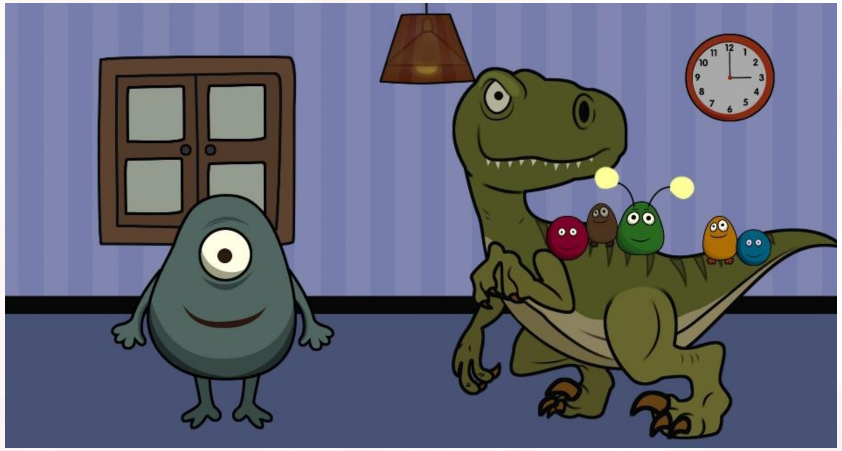

科研论文图像常用的几种图形格式

格式	特点
png	PNG开发的目的是试图替代GIF和TIFF文件格式，同时增加一些GIF文件格式所不具备的特性。具有高保真性、透明性及文件较小等特性，被广泛应用于网页设计、平面设计中。

在介绍文件格式之前，首先要明确作图的用途，不同的用途对应不同的色彩模式。

色彩模式

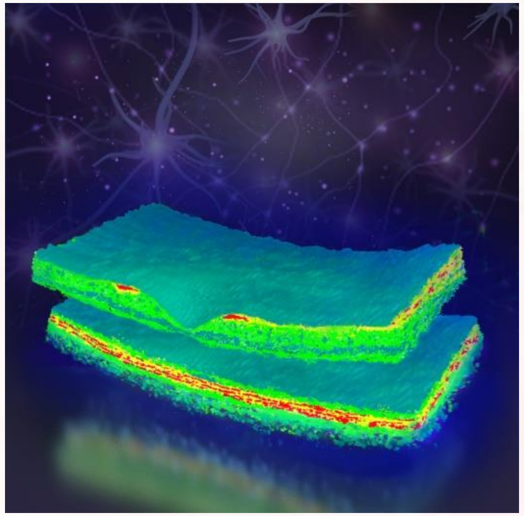

RGB

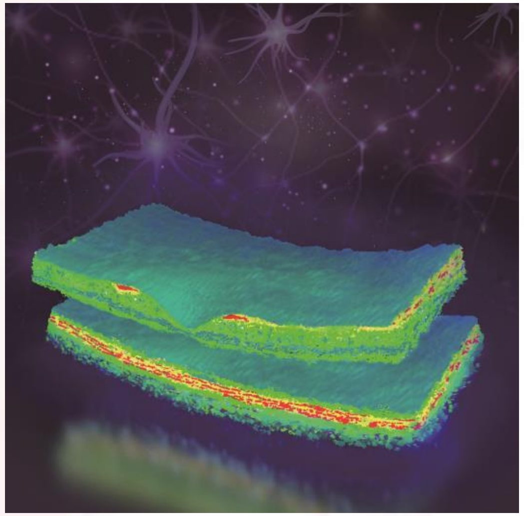

CMYK

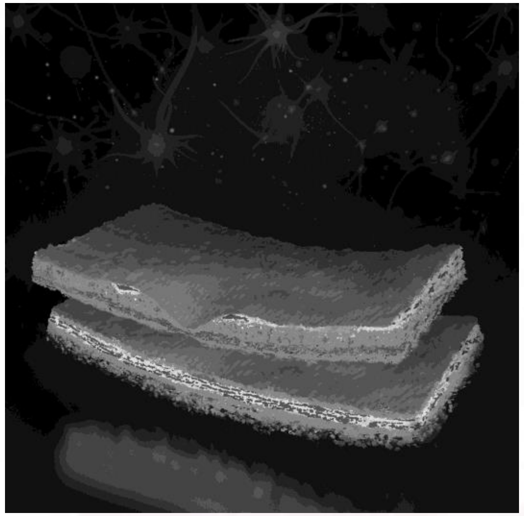

灰度图

索引模式 Lab模式 HSB

灰度图 RGB CMYK

印刷色彩模式，顾名思义就是用来印刷的。

CMYK：青色（C） 洋红色（M） 黄色（Y） 黑色（K）

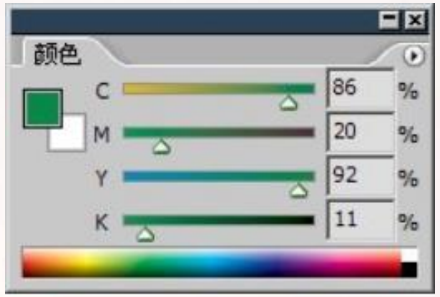

	原理	特点	适用期刊
RGB	发光的 色彩模式	运用于 屏幕显示	电子期刊 纸质期刊
CMYK	反光的 色彩模式	运用于 印刷色彩	纸质期刊
CMYK 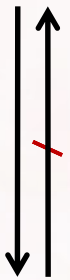 RGB	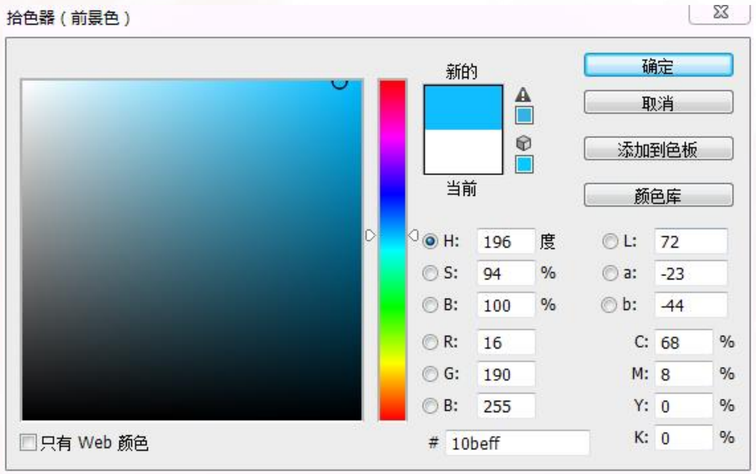		

科研图像思路与规范

每本期刊的专业不同、风格不同、对图片的要求也不同，因此，做必要的调研，信息收集，弄清要求有的放矢。

科研图像思路与规范

2019-Volume58
Angewandte Chemie

2019-Volume9
Theranostics

版式

在出版社的Guide for Authors中会有对图像尺寸的要求，有些出版社也许没有明确列出。这里建议作者向出版社询问，表达自己对文章的重视、专业和细心。

配图版式

封面版式

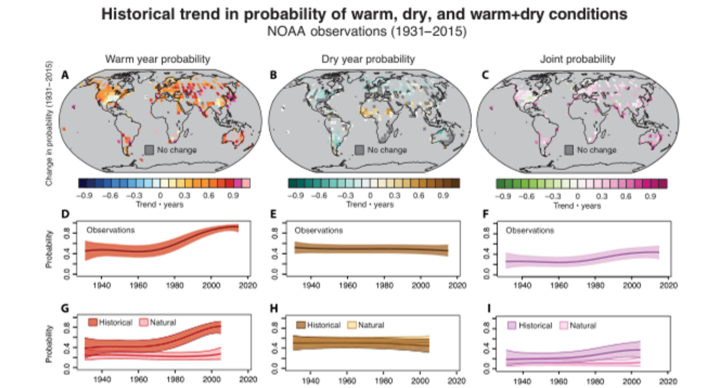

Fig. 1. Historical changes in warm year probability, dry year probability and joint probability. (**A** to **C**) Change in warm year probability, dry year probability, and joint probability, calculated as the trend over the period (1931–2015) using Sen's slope estimator times the length of the period. Maps show results for the 50th percentile of the Bayesian sampling. Dark gray indicates no change in the location parameter through time (see Materials and Methods). (**D** to **F**) Global average of the warm year probability, dry year probability, and joint probability aggregated across the grid points in the National Oceanic and Atmospheric Administration (NOAA) observations. The bold line shows the posterior mean, and the color envelope shows the 2.5th to 97.5th percentile range (see Materials and Methods). (**G** to **I**) Global average of the warm year probability, dry year probability, and joint probability aggregated across the grid points in the Historical and Natural forcing experiments of the CMIP5 global climate model ensemble. The bold line shows the ensemble-mean posterior mean, and the color envelope shows the ensemble-mean 2.5th to 97.5th percentile range (see Materials and Methods).

around 20% (relative to a given area's 1961–1990 mean) throughout the Natural ensemble, with the 2.5th to 97.5th percentile confidence intervals of the Historical and Natural ensembles remaining completely separated after ~1970. There is thus high statistical confidence that the observed increase in warm year probability would not have occurred without anthropogenic forcing.

In contrast, the probability of dry years has remained ~50% at the global scale throughout the observational period (relative to the 1961–1990 baseline; Fig. 1E), with areas of the tropics and subtropics exhibiting increases and much of the extratropics exhibiting decreases or no change (Fig. 1B). Although both the observations and the Historical climate model ensemble exhibit slight indications of a decrease in dry year probability in the late 20th and early 21st centuries, the 2.5th to 97.5th percentile confidence intervals of the Historical and Natural ensembles overlap substantially throughout the historical period (Fig. 1H).

Despite the spatial heterogeneity of trends in dry year probability (Fig. 1B), the increasing trends in warm year probability (Fig. 1A) lead to broad increases in the probability of years that are both warm and dry ("warm+dry"; Fig. 1C). At the global scale, the aggregated warm+dry probabilities are similar to what would be expected from the product of the two univariate probabilities (Fig. 1, D and E), with global warm+dry probability equaling ~20% in the mid-20th century and ~40% in the early 21st century (relative to the 1961–1990 baseline; Fig. 1F). At the regional scale, the largest increases in warm+dry probabilities are generally associated with the largest increases in warm year probabilities, although the lack of data in the tropics likely limits the number of grid points that exhibit increases in both univariate probabilities. The most prominent exception to the general increase in warm+dry probability is the well-documented "warming hole" over the central and southeastern United States, where the warm, dry, and warm+dry probabilities all exhibit decreasing trends over the 1931–2015 period (Fig. 1C).

The increase in global warm+dry probability would be expected to increase the odds that different regions experience warm+dry years simultaneously. Given the negative impacts of co-occurring warm+dry conditions on agricultural yields (*21*) and the importance of co-occurring yield shocks for regional and global agricultural markets [e.g., (*3–5*)], we quantify the joint probability of warm+dry conditions in pairs of global crop and pasture regions (see Materials and Methods). We find that these regions have become substantially more likely to experience warm+dry anomalies in the same year over the historical period (Fig. 2).

Previous work shows that the occurrence of extreme years—and especially extremely warm years—is particularly important for the volatility of agricultural yields and hence prices [e.g., (*5, 22*)]. We therefore analyze the joint probability of progressively larger climate anomalies. Like the co-occurrence of years that are warmer and drier than the historical mean (Fig. 2), we find that the joint probability of simultaneous occurrence of these more extreme combinations of

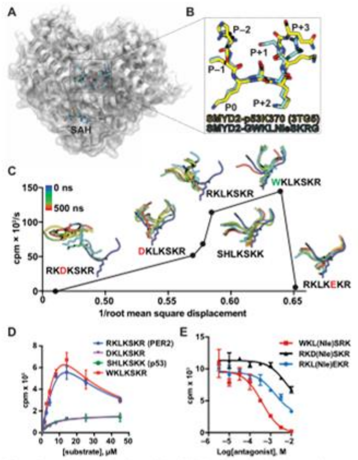

Fig. 4. Structural and kinetic analysis of SMYD2. (**A**) Hybrid ribbon-surface representation of SMYD2 (white) bound to SAH and GWKLNleSKRG (Nle, norleucine) (blue sticks). Costructure has been deposited in the Protein Data Bank (PDB) as PDB: 6MON. (**B**) Overlay of peptide substrates from SMYD2-GWKLNleSKRG (PDB: 6MON) and SMYD2-p53K370 (PDB: 3TG5) structures. (**C**) Scatterplot comparing the relationship between the methylation rate calculated from Fig. 2F and the dynamics of substrate coordination by SMYD2. Root mean square displacement (RMSD) of the Cα atoms of the indicated peptides was calculated from 500-ns whole-atom MD simulations. Peptide orientations at several time points over the course of the MD simulations are shown, indicated by color with the corresponding color scale (top left). (**D**) Kinetic analysis of SMYD2 methylation of p53, PER2, and PER2 derivative substrates. Data points are the mean of three independent measurements, and error is presented as ±SEM. PER2 and WKLKSKR were fit to a substrate inhibition kinetic model. DKLKSKR and SHLKSKK were fit to a standard Michaelis-Menten (MM) model. (**E**) IC_{50} (median inhibitory concentration) measurements of Nle peptide inhibitors of SMYD2 using PER2 as a substrate. Data points are the mean of three independent measurements, and error is presented as ±SEM.

Nle derivatives were less effective, as predicted by K-OPL analysis. However, although RKLKEKR and RKDKSKR were equally poor SMYD2 substrates (Fig. 2F), RKLNleEKR was a more efficient competitive inhibitor than RKDNleSKR (Fig. 4E). This result was consistent with the MD simulation that showed that RKLKEKR formed a more stable complex with SMYD2 (Fig. 4C). Overall, these results suggest that optimal substrates identified by K-OPL screens can serve as scaffolds for further optimization toward more potent inhibitors.

Using K-OPL to identify new SMYD2 substrates

To identify new KMT substrates, we developed a lowest bin (LoB) scoring function based on K-OPL selectivity profiles to rank lysine-centered 7-mer sequences from annotated proteomes. LoB scores are equal to the raw signal from the lowest K-OPL set used to construct an entire 7-mer sequence, e.g., consider PER2 K798 (RKLKSKR). The score for this sequence is assigned by the arginine in the P–3 position, as this set has the lowest signal in this sequence (fig. S1, E and F). The LoB score was purposely designed to minimize false positives and contains no positional weighting common to other motif scoring functions (*27, 28*).

A candidate list of six proteins (PER2, PRDM11, CDC5L, GDAP1, ZPK, and ATP6V1G3) from the top 50 LoB-scored sequences (table S2) was selected for in vitro validation as SMYD2 substrates. All six proteins were methylated by SMYD2 (Fig. 5A and fig. S5A). ZPK and GDAP1 were poor SMYD2 substrates (fig. S5A). Available structural data for ZPK showed that the target lysine is in a structured helix that likely prohibited methylation by SMYD2 (fig. S5B), but no structural data were available to rationalize why GDAP1 is not a more robust SMYD2 substrate. To determine whether the lysine predicted by the K-OPL screen was methylated, we generated protein substrates with the target lysine substituted to arginine (K to R). All K to R mutant substrates had reduced methylation (Fig. 5A and fig. S5A). For CDC5L, ATP6V1G3, and PER2, the K to R mutation did not completely abolish methylation, suggesting that additional residues are also being methylated. Consistent with rate measurements for the MAPKAPK3 K355 peptide (Fig. 2F), methylation of full-length recombinant MAPKAPK3 was weaker than most of the newly identified SMYD2 substrates (Fig. 5A), requiring a much longer exposure to detect methylation of this protein (fig. S5A).

Overall, SMYD2 methylated four of the newly identified substrates (PER2, PRDM11, CDC5L, and ATP6V1G3) at least as efficiently as the known substrate, p53. These results validate the use of K-OPL selectivity profiles to identify new KMT substrates.

K-OPL analysis predicts the impact of missense mutations on substrate usage

Missense mutations have been shown to alter kinase signaling networks, including mutations that cause amino acid substitutions in proximity to the modified residue (*29*). We sought to determine whether K-OPL selectivity profiles could predict the impact of missense mutations on a KMT substrate at the protein level. Guided by the SMYD2 K-OPL profile, we generated a PRDM11 mutant (K89D), predicted to render this robust SMYD2 substrate deficient. In an in vitro KMT assay, PRDM11 K89D methylation was reduced compared to the wild-type PRDM11 (Fig. 5B). In addition, mutations predicted to enhance methylation of the weak SMYD2 substrate MAPKAPK3 (D353R and T356S) improved methylation of this protein (Fig. 5B). These results show that K-OPL–derived selectivity profiles accurately predict how single amino acid changes near the target lysine can significantly affect the efficiency of a KMT substrate at the protein level.

We next turned our attention to predicting how reported missense mutations in primary human cancer sequencing datasets might rewire lysine methylation signaling networks because of substitutions within SMYD2 substrate motifs. To do so, we catalogued and analyzed K-centric 7-mer amino acid sequences on a proteome-wide scale. Comparison of the LoB scores for SMYD2 targets in the normal proteome (UniProt) with the oncoproteome (COSMIC) (*30*) resulted in the identification of four classes of missense mutations that may affect SMYD2 lysine methylation signaling. The four classes include mutations that (i) weakened, (ii) strengthened, (iii) created, or (iv) had no effect on a target of methylation (Fig. 5C and table S3). These

出版社	单栏宽度（cm）	双栏宽度（cm）
RSC	8.3 cm	17.1 cm
WILEY	8.5 cm	17.8 cm
Nature	8.9 cm	18.3 cm
APS	8.6 cm	17.8 cm

总结：一般期刊的单栏图像宽度为8 cm-9 cm，双栏17 cm -18 cm左右，高度一般不固定，需具体期刊具体对待。

科研图像思路与规范


RSC Sample Cover
Safe area:
All important details should remain inside the PINK dotted line
Background area: All background should extend to, but not past the BLUE dotted line


ChemComm

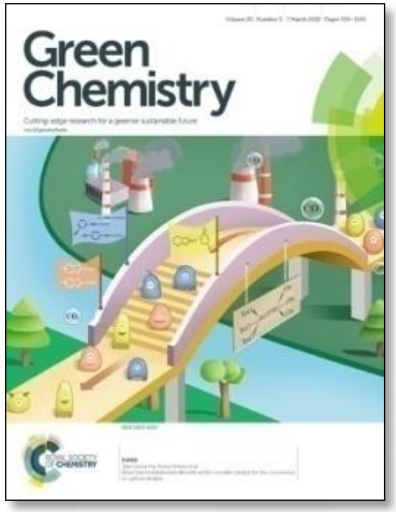
Green Chemistry

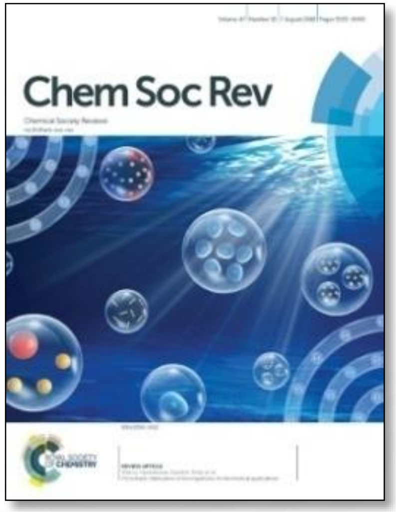
Chem Soc Rev

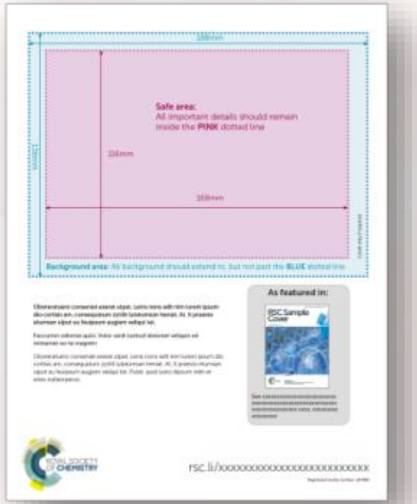
Safe area:
All important details should remain inside the PINK dotted line
Background area: All background should extend to, but not past the BLUE dotted line
As featured in:


As featured in:
rsc.li/catalysis


As featured in:
rsc.li/materials-a

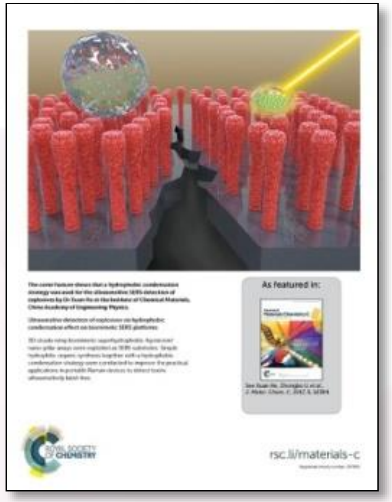
As featured in:
rsc.li/materials-c

COVER IMAGE SIZES

Journal Name	ID	Width(in)	Height(in)	W(cm)	H(cm)	Notes
ACS Biomaterials Science & Engineering	AB	8.19	10.00	20.80	25.40	title covers top 1.7" of image
Analytical Chemistry	AC	8.19	10.00	20.80	25.40	title covers top 2.2" of image
ACS Applied Energy Materials	AE	8.19	8.47	20.80	21.51	
ACS Applied Materials & Interfaces	AM	8.19	8.47	20.80	21.51	
ACS Applied Nano Materials	AN	8.19	8.47	20.80	21.51	
ACS Applied Polymer Materials	AP	8.19	8.47	20.80	21.51	
Accounts of Chemical Research	AR	8.19	10.00	20.80	25.40	title covers top 2" of image
Bioconjugate Chemistry	BC	8.19	7.48	20.80	19.00	
Biochemistry	BI	8.19	10.00	20.80	25.40	title covers top 3" of image
Biomacromolecules	BM	7.00	7.00	17.78	17.78	
ACS Chemical Biology	CB	8.19	10.00	20.80	25.40	title covers top 3" of image
Journal of Chemical Information and Modeling	CI	8.19	7.70	20.80	19.56	
Chemistry of Materials	CM	7.19	7.62	18.26	19.35	
ACS Chemical Neuroscience	CN	8.19	10.00	20.80	25.40	
Chemical Reviews	CR	8.19	10.00	20.80	25.40	title covers top 2.5" of image
ACS Catalysis	CS	6.88	7.75	17.46	19.69	
Journal of Chemical Theory and Computation	CT	6.79	7.10	17.25	18.03	

AI 出图

PS出图

dpi： DOTS PER INCH

$$\text{分辨率} = \frac{\text{像素（宽）} \times \text{像素（高）}}{\text{宽度} \times \text{高度}}$$

$$\text{图像大小} = \frac{\text{像素（宽）} \times \text{像素（高）}}{\text{分辨率} \times \text{（宽度×高度）}}$$

Please send your suggestions for cover pictures or frontispieces directly to the Editorial Office. Please send a TIFF file at 300 dpi. Please use CMYK colors, otherwise they may not reproduce as intended.The circle on the cover of Angewandte has a diameter of 16.5 cm (6.5 in). Please also send an explanatory text of no more than 500 characters. (Examples)For a review, minireview or communication frontispiece, the diameter is 18.5 cm (7.28 in). The latter should contain some text to arouse the readers' interest (84 mm wide, 7 lines).

版式	a diameter of 16.5 cm
分辨率	300dpi
保存格式	TIFF
色彩模式	CMYK

小结

在现代科研中，论文配图水平的高低直接影响到文章质量的好坏。在摄影风格、三维风格、平面风格的图像中，多数文章插图是在平面软件PS、AI中完成的，封面文章配图多数是在三维软件中复杂建模完成，不同期刊对于文章及图片输出格式要求不同，在理解的基础上准确提供文章配图的分辨率、保存格式、色彩模式。

谢 谢 大 家 ！

图形图像处理学习讨论群